Solitary pulse shaping dynamics in cavity-dumped laser oscillators

Alexander Killi and Uwe Morgner

Max Planck Institute for Nuclear Physics, Saupfercheckweg 1, D-69117 Heidelberg, Germany
A.Killi@mpi-hd.mpg.de

Abstract: The pulse shaping dynamics of a diode-pumped laser oscillator with cavity dumping operating in the solitary regime is studied experimentally and numerically. The stability of the laser system is investigated in dependence on the relevant laser parameters. With a stroboscopic detection technique the intracavity temporal and spectral pulse profiles are measured between two dumping events. The results are compared to the numerical analysis of the system. Due to the strong periodic disturbance of the solitary pulse imposed by the dumping process a second set of Kelly-side bands can be identified.

OCIS codes: (140.3580) Lasers, solid-state; (140.4050) Mode-locked lasers; (140.3480) Lasers, diode-pumped; (320.7090) Ultrafast lasers; (320.7160) Ultrafast technology

References and links

1. M. Ramaswamy, M. Ulman, J. Paye, and J. G. Fujimoto, "Cavity-dumped femtosecond Kerr-lens mode-locked Ti:Al2O3 laser," Opt. Lett. **18**, 1822-1824 (1993)
2. A. Baltuska, Z.Wei, M. S. Pshenichnikov, D. A. Wiersma, and R. Szipöcs, "All solid-state cavity dumped sub-5-fs laser," Appl. Phys. **B 65**, 175-188 (1997)
3. M. S. Pshenichnikov, W. P. d. Boeij, and D. A. Wiersma, "Generation of 13-fs, 5-MW pulses from a cavity-dumped Ti:sapphire laser," Opt. Lett. **19**, 572-574 (1994)
4. S. Schneider, A. Stockmann, and W. Schuesslbauer, "Self-starting mode-locked cavity-dumped femtosecond Ti:sapphire laser employing a semiconductor saturable absorber mirror," Opt. Express **6**, 220-226 (2000)
5. A. Killi, U. Morgner, M. J. Lederer, and D. Kopf, "Diode-pumped femtosecond laser oscillator with cavity dumping," Opt. Lett. **29**, 1288 (2004)
6. X. Liu, D. Du, and G. Mourou, "Laser ablation and micromachining with ultrashort laser pulses," IEEE J. Quantum Electron. **QE-33**, 1706-1716 (1997)
7. R. Osellame, S. Taccheo, M. Marangoni, R. Ramponi, P. Laporta, D. Polli, S. D. Silvestri, and G. Cerullo, "Femtosecond writing of active optical waveguides with astigmatically shaped beams," J. Opt. Soc. Am. B **20**, 1559-1567 (2003)
8. R. Osellame, N. Chiodo, G. D. Valle, R. Ramponi, G. Cerullo, A. Killi, U. Morgner, M. Lederer, and D. Kopf, "Optical waveguide writing with a diode-pumped femtosecond oscillator," Opt. Lett. (in press) (2004)
9. S. M. Kelly, "Characteristic sideband instability of periodically amplified average soliton," Electron. Lett. **28**, 806-807 (1992)
10. T. R. Schibli, E. R. Thoen, F. X. Kärtner, and E. P. Ippen, "Suppression of Q-switched mode locking and break-up into multiple pulses by inverse saturable absorption," Appl. Phys. **B70**, S41 (2000)
11. F. X. Kärtner and U. Keller, "Stabilization of solitonlike pulses with a slow saturable absorber," Opt. Lett. **20**, 16-18 (1995)
12. F. X. Kärtner, L. R. Brovelli, D. Kopf, M. Kamp, I. Calasso, and U. Keller, "Controll of solid-state laser dynamics by semiconductor devices," Opt. Eng. **34**, 2024-2036 (1995)
13. G. P. Agrawal, *Nonlinear Fiber Optics* (Academic Press, San Diego, 1995)
14. S. Chenais, F. Druon, F. Balembois, P. Georges, R. Gaume, P. H. Haumesser, B. Viana, G. P. Aka, and D. Vivien, "Spectroscopy and efficient laser action from diode pumping of a new broadly tunable crystal: Yb 3+ : Sr 3 Y (BO 3) 3," J. Opt. Spc. Am. B **19**, 1083-1091 (2002)
15. D. J. Jones, Y. Chen, H. A. Haus, and E. P. Ippen, "Resonant sideband generation in streched-pulse fiber lasers," Opt. Lett. **23**, 1535 (1998)

#4389 - $15.00 US Received 17 May 2004; revised 12 July 2004; accepted 13 July 2004

16. N. J. Smith, K. J. Blow, and I. Andonovic, "Sideband Generation Through Perturbations to the Average Soliton Model," IEEE J. Lightwave Technol. **10**, 1329-1333 (1992)

1. Introduction

Cavity dumping of mode-locked laser oscillators is a simple and effective scheme to increase the pulse energy at the expense of pulse repetition rate without employing complex amplifiers. The use of cavity-dumped femtosecond lasers has been investigated intensively over the last decade [1-4]. However, to our knowledge no systematic analysis of the pulsing dynamics has been performed so far. This is quite surprising since these lasers exhibit a variety of stable and unstable operating states. To identify the useful parameter ranges a detailed experimental and numerical study of a cavity-dumped laser is presented in this paper. Recently, we demonstrated a directly diode-pumped Yb:glass based setup [5]. Such a system offers pulse energies close to the micro joule range from a compact, robust and simple setup, which is of interest for various industrial and scientific applications [6, 7]. In particular our laser system was used successfully for waveguide writing in glass [8].

The diode-pumped solitary mode-locked laser oscillator incorporates some inherent time constants such as the gain relaxation period and the soliton period. Cavity dumping results in an additional periodic perturbance of the solitary pulse. Since all three time constants can be in the same order of magnitude, such a system displays an extraordinary dynamic behavior in certain parameter ranges and a detailed knowledge about the pulsing dynamics is necessary for the identification and anticipation of stable regimes. Furthermore, since cavity dumping represents a periodic perturbance of the solitary pulse, the intracavity pulse shaping transient from one dumping event to the next can be studied in detail – at least in the stable regimes. In this paper we will compare the transient measurements to corresponding solutions of the master equation of mode-locking. The excellent agreement between the measurement and the theory allows extrapolating the pulse parameters beyond the limits of the current experiment. The paper is organized as follows: After a brief description of the laser setup, we introduce three dynamic regimes which are dependent on different dumping frequencies. The pulse to pulse stability, the transient spectra and autocorrelations are discussed with respect to the theoretical model. A numerical evaluation of the laser dynamics is carried out and compared to the experimental results. The major pulse shaping mechanism is shown to be caused by solitary pulse propagation while the spectral properties of the laser pulses are strongly influenced by the generation of Kelly sidebands [9].

2. Description of laser setup

The laser in our experimental set-up is an Yb:glass femtosecond oscillator, which is described in detail in [5]. It consists of a standard z-shaped cavity, stretched to a length of 7.1 m. The Yb:glass was pumped by a laser diode at 976 nm with 5.2 W of pump power. The laser was operated in the solitary regime. It employed dispersive mirrors and was mode-locked by a saturable semiconductor absorber mirror (SESAM). In the unperturbed case (without cavity dumping) the typical laser was operated at a repetition frequency of 21 MHz with intracavity pulse energy of 700 nJ. It had a spectral width of 4 nm at a center wavelength of 1040 nm, and with a pulse length of 300 fs it was almost transform limited (assuming sech^2). The dispersion was adjusted to give the shortest pulse possible and it was found that any less negative dispersion led to multiple pulsing. We used an electro-optical modulator (EOM) based on BBO in combination with a thin film polarizer (TFP) as a cavity dumper. Dumping ratios of up to 50% could be achieved at repetition frequencies of up to 200 kHz, limited by the speed of the high voltage switches of the EOM. The intracavity transients were observed by detecting the light leakage of a cavity mirror. By generating the second harmonic in a 300 µm thick $KNbO_3$-crystal both, the energy and peak power evolution were monitored simultaneously.

#4389 - $15.00 US Received 17 May 2004; revised 12 July 2004; accepted 13 July 2004

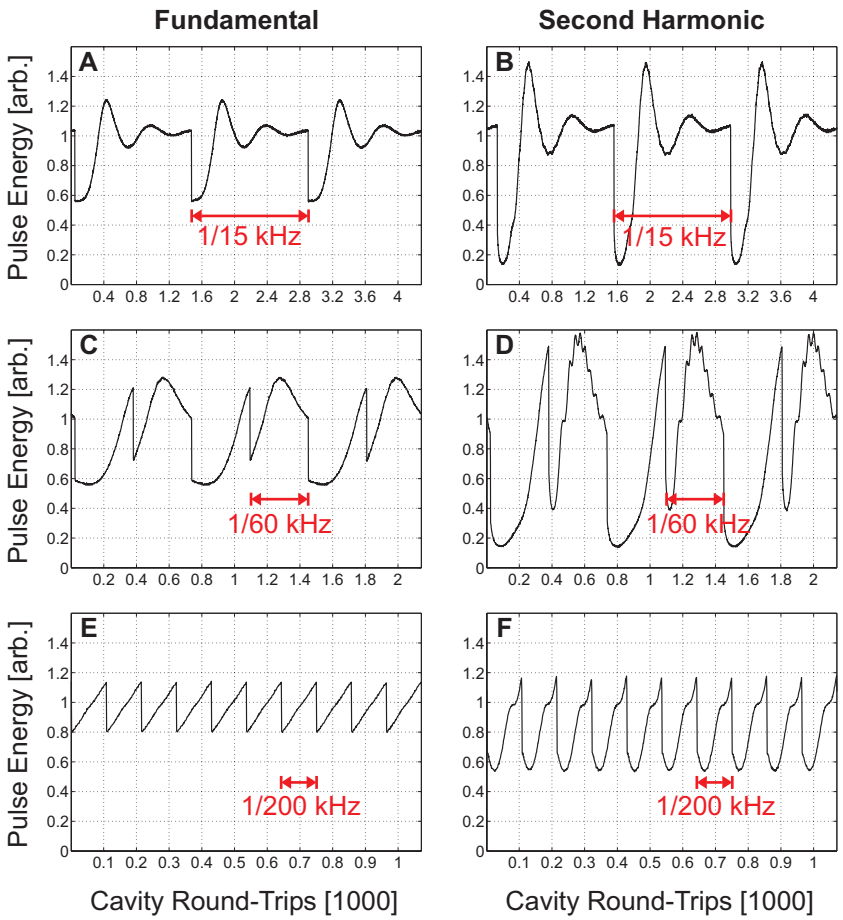

Fig.1. Intracavity energy and peak power (detected via second harmonic energy) as monitored by a photo diode. The red arrows indicate the dumping period.

3. Stability considerations

In order to characterize our laser in terms of stability, the system was analyzed in different operational regimes. The dynamic behavior can be classified into three different regimes which we will refer to as 'relaxed', 'intermediate', and 'transient' regime for low, medium and high dumping rates respectively. Typical pulse energy and peak power evolutions between two dumping events are shown in Fig. 1.

For low repetition rates (<20kHz, Fig. 1(A, B)) the time between the dumping is long compared to the period of the relaxation oscillations which allows the laser to relax to its steady state. In terms of pulse duration and chirp, the dumped pulses correspond to the unperturbed laser without cavity dumping. It is possible to extend the 'relaxed' regime to rather high frequencies (up to 20 kHz) by operating the system in terms of power and dispersion very close to the multiple pulse break-up. The overshoot after the dumping is limited considerably due to the optimized ratio between spectral filtering and absorber action, as was analyzed in detail in [10]. In this regime the observed pulse to pulse reproducibility is very high. The rms-noise of the energy fluctuations is better than 0.1% which is the resolution limit of the used oscilloscope.

In the 'intermediate' regime with a dumping rate close to the relaxation oscillation frequency (around 40 kHz), a double-energy state for subsequent pulses appears and

#4389 - $15.00 US
Received 17 May 2004; revised 12 July 2004; accepted 13 July 2004

subharmonic behavior is observed. Intracavity pulse energy and peak power evolution between the dumping events in this regime are shown in Fig. 1(C, D). This regime extends more or less from 20 to 80 kHz. The secondary oscillations visible on the crest of the peak power transient waveform are an effect of the third relevant time constant, namely the soliton period which becomes important in the third, the 'transient' regime.

The 'transient' regime is present at dumping frequencies higher than 80 kHz; the laser has no time to relax before the next dumping occurs. This is depicted in Fig. 1(E, F). Despite the saw tooth shape of the fundamental, the structured second harmonic trace which reveals oscillations in the pulse duration indicates the soliton period. As will be shown in the following, these oscillations can have a major effect on the stability of the system.

To illustrate the complex interplay between the three relevant time constants in the transient regime, the relaxation oscillation, the soliton period, and the dumping frequency, a stability diagram is measured and given in Fig. 2. As a measure for the stability, the rms-noise of the second harmonic of dumped pulses is plotted as a function of dumping ratio and dumping frequency. Bright regions are operational parameters which lead to high stability, whereas dark regions represent poor stability. At certain dumping frequencies with high stability the pulse to pulse rms-noise is better than 0.8%. It is obvious that a decreasing dumping ratio diminishes the perturbance and increases the stability, whereas at higher dumping ratios the darker regions of instability become broader, up to the point that only a few narrow stable areas remain. The instability can manifest itself as a subharmonic multi energy-state in the second harmonic signal, irregular energy fluctuations, or both.

The three graphs in the lower part of Fig. 2 show the peak power transients at different dumping frequencies in three neighboring stable areas of the 'transient' regime as indicated in the stability plot. It is clearly visible that distinct regimes can be classified by the number of periods existing in the transient. Since the second harmonic transients unveil the soliton pulse width dynamics, an integer number of soliton periods fitting in the transient is necessary for the stability of the system. For clarification we denote the different regions 'transient' regime TR_n (where n is the number of minima / saddle points in the second harmonic transient).

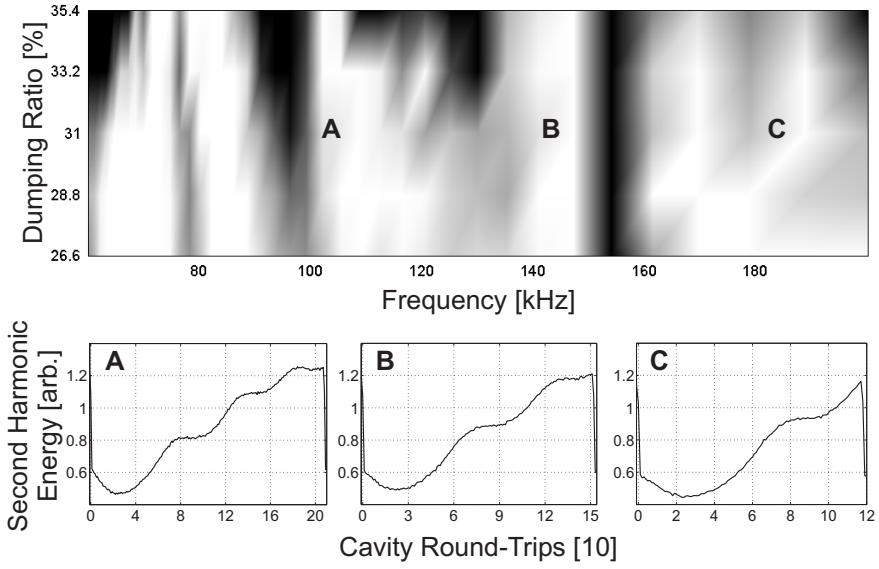

Fig. 2. Upper part: measured stability regions of the system in the transient regime. Bright areas: low rms noise = high dynamical stability; dark areas: poor dynamical stability. Lower part: second harmonic transient signal as monitored by a fast photodiode. The different regimes A (TR_4), B (TR_3), and C (TR_2) are separated by unstable regions.

#4389 - $15.00 US Received 17 May 2004; revised 12 July 2004; accepted 13 July 2004

At high repetition rates the system is in the regime TR_2 (Fig. 2(C)) and by lowering the dumping frequency, the laser becomes unstable in the area of 155 kHz and switches to TR_3 (Fig. 2(B)), where the laser is stable again. The same happens around 120 kHz, where TR_4 is reached as shown in Fig. 2(A). The relaxation oscillation is responsible for a strong destabilization observed below 60 kHz, where we enter the 'intermediate' regime with distinct subharmonic switching of the pulse energy (Compare to Fig. 1(C, D)). The system is unstable until the 'relaxed' regime below 20 kHz is entered.

In contrast to the 'relaxed' case, the characteristics of the dumped pulses in the 'transient' regime are different from the unperturbed case for obvious reasons. The spectral and temporal properties of the dumped pulses are compared in Fig. 3. While the temporal pulse shape and width remain similar, the optical power spectrum in the 'transient' regime is strongly modulated. From the shape of the autocorrelation we conclude that this structure is not due to multiple pulse instability. To clarify the details of the pulse shaping in the 'transient' regime we employed a more sophisticated method to measure transient spectra and autocorrelation traces.

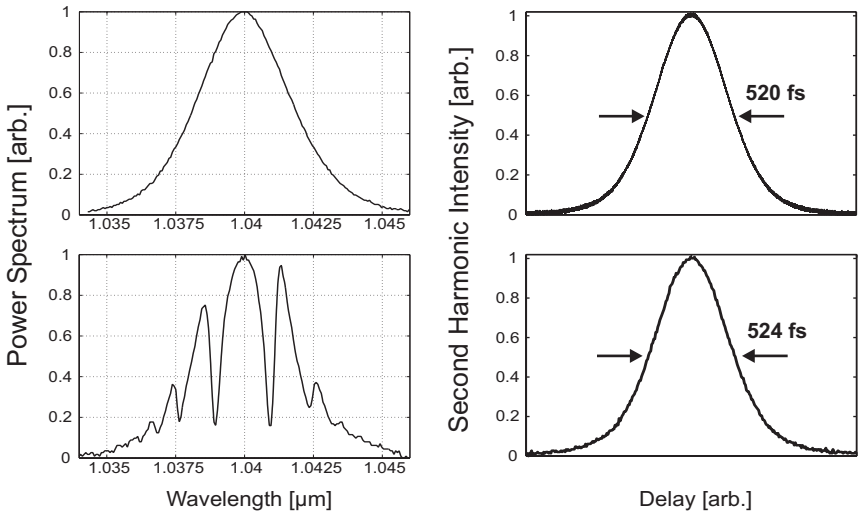

Fig. 3. Measured spectra (left) and autocorrelation traces (right). The upper two plots are taken in the 'relaxed' regime, they correspond to the results without cavity dumping, whereas shown below is the 'transient' regime with a dumping rate of 180 kHz. The autocorrelation width of 520 fs (524 fs) corresponds to a pulse width of 337 fs (340 fs).

4. Measurement setup and experimental results

In order to obtain further insight into the transient dynamics of the laser system, the evolution of the intracavity energy was measured along with its autocorrelation trace and optical power spectrum. To achieve this, the intracavity pulses of the laser system were monitored by a background free autocorrelator and a scanning Fabry-Perot spectrometer. By detecting the output signal of both the autocorrelator and the spectrometer with fast photo diodes, subsequent laser pulses from the oscillator could be resolved. Fig. 4 shows a schematic of the setup. A synchronization signal taken from the cavity dumper driver is used as the sampling clock for the oscilloscope (LeCroy Waverunner LT584). By adjusting the time delay with respect to the dumping event it was possible to record spectrum and autocorrelation trace for each roundtrip. For obvious reasons this method can only be employed in stable regimes where the pulse evolution is reproducible in each dumping cycle.

#4389 - $15.00 US Received 17 May 2004; revised 12 July 2004; accepted 13 July 2004

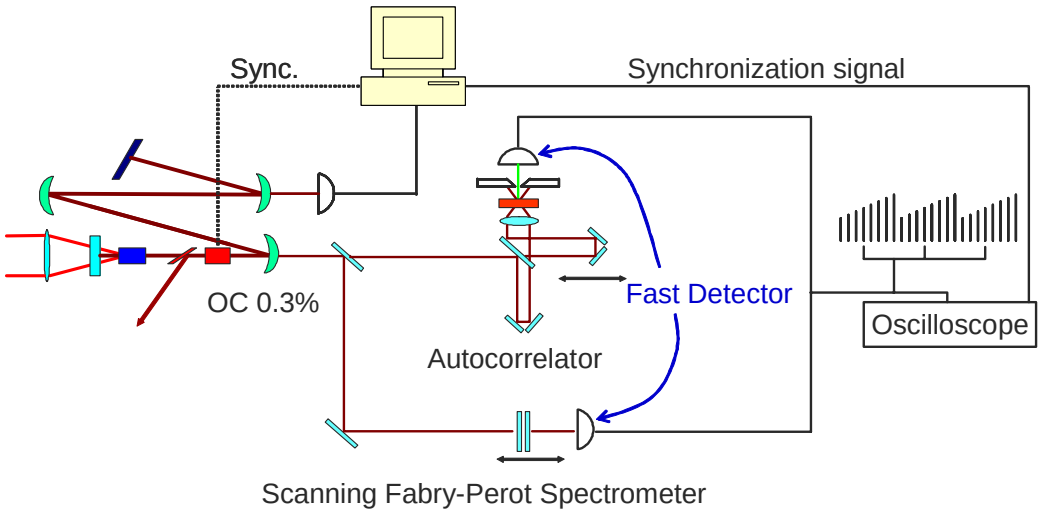

Fig. 4. Experimental setup of the directly diode-pumped Yb:glass laser with cavity dumping, employing a synchronous sampling scheme for autocorrelation and power spectrum of the pulse sequence during the transient.

In Fig. 5 the transients of the autocorrelation and power spectra between two dumping events are shown for a dumping frequency of 180 kHz. Note the well shaped autocorrelation trace despite of the strongly structured spectra. Furthermore an oscillation in the spectral and temporal width of the pulse can be observed. By comparison with Fig. 2(C) we can identify the laser to operate in the TR_2 regime. The periodicity of this oscillation will be discussed in the following section.

The most prominent property in the measured transient optical spectrum is the appearance of spectral sidebands moving towards the center of the spectrum (see the motion sequence). To understand this interesting behavior which was to our knowledge not yet reported in the literature, we employed numerical simulations of the pulse shaping.

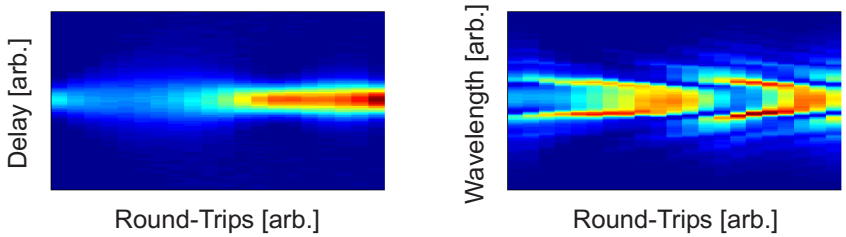

Fig. 5. Measured autocorrelation and power spectrum of the pulse sequence between two dumping events for a dumping frequency of 180kHz. Red color denotes high intensity, blue color low intensity. For a animated sequence showing the measured motion of the spectral sidebands see the attached avi-file. (Movie 342 kB)

5. Numerical simulations

The dynamics of a SESAM mode-locked laser can be described in very good approximation by three differential equations [10-12], for the temporal dynamics of the pulse envelope, the laser gain and the absorber loss. The master equation of mode-locking, describing the evolution of the pulse's envelope reads

#4389 - $15.00 US
Received 17 May 2004; revised 12 July 2004; accepted 13 July 2004

Table 1. Parameter values used in the simulations

Parameter	Value	Parameter	Value
g_0	0.21	E_L	3.8 mJ
l	0.027	E_q	138 nJ
q_0	0.075	τ_L	1.3 ms
Ω_g	$2\pi \cdot 2$ THz	τ_q	1.5 ps
Ω_f	$2\pi \cdot 10$ THz	T_R	45 ns
γ	0.113 / MW	β_2	-7200 fs^2

$$T_R \frac{\partial}{\partial T} A(T,t) = \left[g(T) + D_{g,f} \frac{\partial^2}{\partial t^2} - l - q(T,t) + j \frac{\beta_2}{2} \frac{\partial^2}{\partial t^2} - j\gamma \left| A(T,t) \right|^2 \right] A(T,t).$$

Here, T_R is the cavity round-trip time, $A(T,t)$ is the slowly varying field amplitude normalized in such a way that $|A(T,t)|^2$ represents the instantaneous power as a function of the local time frame t and as well of T, a time variable on the scale of many cavity round-trips. g, l are the round-trip gain and loss respectively. $D_{g,f} = g/\Omega_g^2 + 1/\Omega_f^2$ the gain and spectral filtering. Ω_g is the half-width at half-maximum (HWHM) gain bandwidth and Ω_f is the HWHM filter bandwidth. $q(T,t)$ denotes the saturable absorber loss, β_2 the intra-cavity group delay dispersion (GDD). The self phase modulation (SPM) coefficient γ is given by the nonlinear refractive index n_2, the center wavelength λ_0, the mode area inside the laser glass A_{eff}, and its double pass length ℓ according to $\gamma = 2\pi n_2 \ell / (\lambda_0 A_{\text{eff}})$. The rate equation for the gain dynamics is given by

$$T_R \frac{\partial g(T)}{\partial T} = -T_R \frac{g(T) - g_0}{\tau_L} - g(T) \frac{E_P}{E_L},$$

where τ_L is the upper state lifetime of the laser medium, E_P the pulse energy $E_P = \int_{-T_R/2}^{T_R/2} \left| A(T,t') \right|^2 dt'$, and E_L the saturation energy of the laser medium. The third equation describes the absorber dynamics,

$$\frac{\partial q(T,t)}{\partial t} = -\frac{q(T,t) - q_0}{\tau_q} - q(T,t) \frac{\left| A(T,t) \right|^2}{E_q},$$

where τ_q is the carrier recovery time, E_q the saturation energy, and q_0 the non-saturated loss of the absorber.

These equations have been integrated by the split-step Fourier method [13]. The parameters used for the simulations are either determined by the setup or taken from [14] and are summarized in table 1. The result for a dumping frequency of 180 kHz is depicted in Fig. 6. A good agreement of the spectral and pulse evolution between the simulation and the experiment in Fig. 5 can be observed.

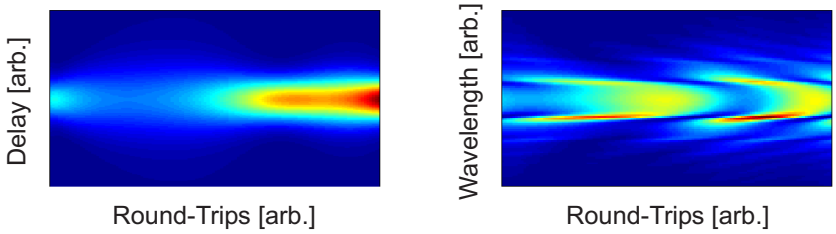

Fig. 6. Simulated autocorrelation and power spectrum of the pulse sequence between two dumping events at a dumping frequency of 180kHz. Red color denotes high intensity, blue color low intensity. For an animated sequence showing the calculated motion of the sidebands see the attached avi-file. (Movie 846 kB)

#4389 - $15.00 US Received 17 May 2004; revised 12 July 2004; accepted 13 July 2004

To stress this even further, the simulated (red) and the measured (blue) spectra directly before the dumping are compared in Fig. 7. The agreement is excellent, and we can therefore conclude that our laser system is indeed very well described by the above equations.

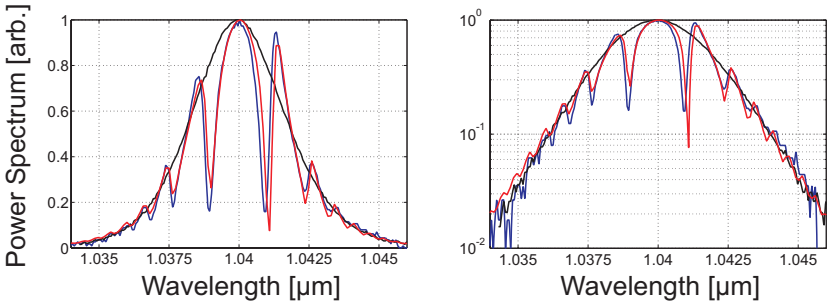

Fig. 7. Linear and logarithmic plots of the spectra immediately before the dumping event, at 180kHz repetition rate; red: simulation; blue: measurement. The black curve is the measurement of the unperturbed laser.

Fig. 8 shows the simulated power spectrum and intensity of the pulse over a larger range on a logarithmic scale along with the corresponding phase. The remote sidebands in the power spectrum are identified as the well known Kelly-sidebands due to the perturbation of the soliton with the periodicity of the oscillator round trip frequency [9, 15, 16]. The dips in the chirped temporal continuum background and the sidebands close to the peak of the spectrum (see also Fig. 7) are a result of the dumping. The simulations reveal that these sidebands are due to the periodic perturbance of the system on a timescale much larger than the cavity round-trip time.

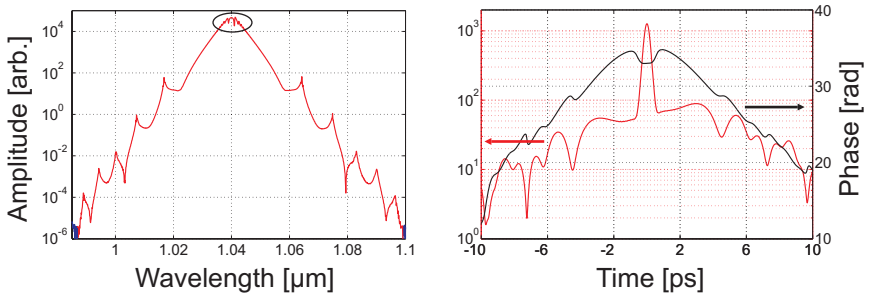

Fig. 8. Simulated pulse spectrum (left) and pulse envelope (right, red) and phase (black) immediately before the dumping event at 180kHz repetition rate. The ellipse marks the dominant spectral structures, which are shown in more detail in Fig. 7.

6. Discussion

As was pointed out in the previous section, the laser system imposes two dominant perturbation periodicities on the pulse. One is the cavity round-trip time wherein we expect the 'standard' Kelly sidebands. They appear at a spectral position where the nonlinear phase shift per round-trip modulo 2π is equal to the linear cavity phase due to dispersion. At these spectral positions, constructive interference of the pulse with the dispersive background occurs and phase matched continuum is generated at certain spectral positions where sidebands can build up with time. This is illustrated in the left part of Fig. 9: Exactly at the points of intersection between the phase parabola due to the strong negative roundtrip dispersion and the nonlinear phase modulo 2π, a sideband is present in the (calculated) optical spectrum. The "standard" Kelly sidebands have not been observed in the experiment because of the limited dynamics of the used spectrometer.

On the second timescale, namely the dumping period – much longer than the cavity round-trip time – a second set of sidebands becomes apparent. As the pulse accrues a lot more

#4389 - $15.00 US Received 17 May 2004; revised 12 July 2004; accepted 13 July 2004

dispersion between two dumping events, the phase parabola of the cavity dispersion is much steeper and the sidebands appear much more pronounced around the center of the spectrum. The right part of Fig. 9 compares measured and calculated optical power spectra before dumping with the cavity phase. The sidebands appear exactly at the intersections between the phase parabola and the nonlinear phase modulo 2π, as predicted by theory.

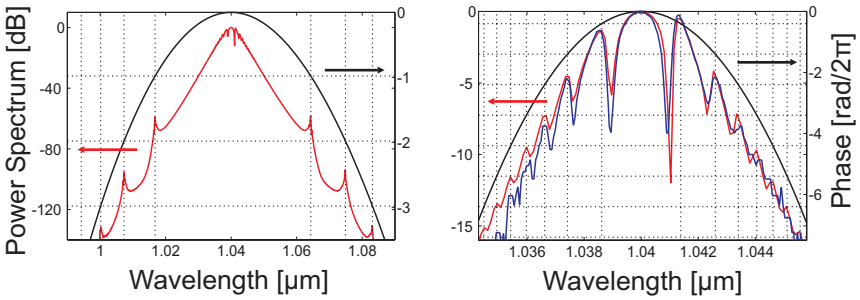

Fig. 9. Phase matching between linear and nonlinear phase. The matching points become apparent in the optical spectrum as small peaks (Kelly sidebands). Left: Sidebands due to the cavity round-trip periodicity. Right: Sidebands due to the dumping period. Red curves show the simulated spectra, whereas the blue curve shows the corresponding measurement. The cavity phase parabola is given by the solid black curve, the nonlinear phase modulo 2π by the dotted horizontal lines. The vertical dotted lines indicate phase matching between the nonlinear and the linear phase, coinciding with the spectral peaks.

A simple control of the Kelly sidebands can be accomplished by changing the dumping frequency. If the dumping frequency is increased a reduced cavity GDD per dumping cycle results and therefore a shifting of the Kelly sidebands away from the center of the spectrum, as is illustrated in Fig.10 for dumping frequencies of 540 kHz, 880 kHz, and a dumping ratio of 40%. The simulation reveals that the sidebands become less pronounced with higher dumping frequencies due to the less efficient coupling to the continuum radiation.

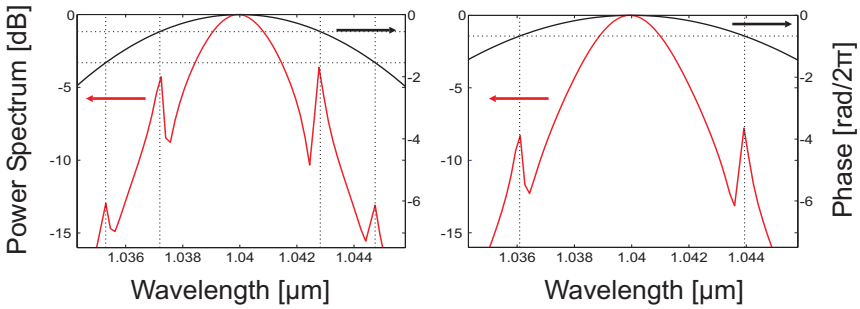

Fig.10. Spectral modulation for different dumping frequencies. Left: 540 kHz; Right: 880 kHz. The cavity phase is given by the solid black curve, the nonlinear phase by the dotted horizontal lines. The dumping ratio is 40%.

The operation at higher dumping frequencies is also preferable in terms of stability. With a dumping frequency of more than 500 kHz which is well beyond the relaxation oscillation (on the order of some 10 kHz) and the phase periodicity of the soliton (on the order of some 100 kHz), the system is in the stable TR_1-regime. To anticipate the laser performance with high dumping rates the stability for varying dumping rates in the range of 80 kHz up to 2 MHz and dumping ratios in the range of 0.2 up to 0.4 has been analyzed with the numerical simulation. The results are shown in Fig.11. Again the TR_n regimes can readily be identified. We find good stability at frequencies of up to 1 MHz. The instable region (shown in black) at very high frequencies is caused by the additional losses of the cavity dumping resulting in a significant drop in the average pulse energy and Q-switching instabilities. This can be compensated for by a stronger pump.

#4389 - $15.00 US
Received 17 May 2004; revised 12 July 2004; accepted 13 July 2004

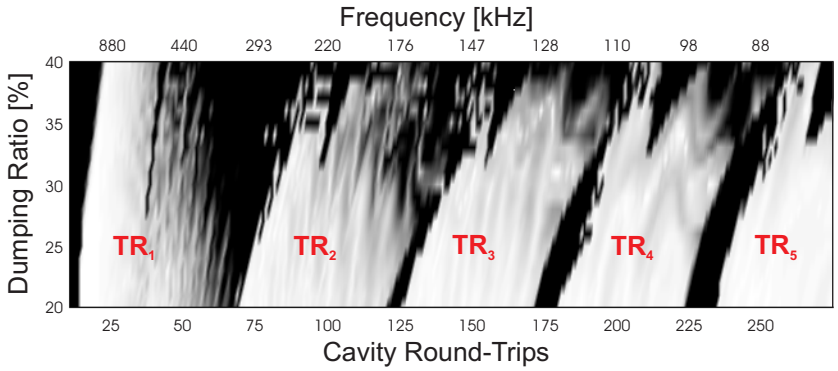

Fig. 11. Stability regions of the system as predicted by simulation. Bright areas: low rms noise = high dynamical stability; Dark areas: poor dynamical stability. Upper horizontal axis: dumping frequency. Lower horizontal axis: number of roundtrips between dumping events at 22 MHz fundamental repetition frequency of the oscillator.

The inward motion of the spectral sidebands during the transient (see Fig. 6 and the added multimedia file), can be well understood by the increasing intracavity power and the resulting change in the nonlinear phase shift. The movement of the spectral sidebands is accompanied by an oscillation of the pulse width, as shown in detail in Fig.12. The figure shows both the transient peak power and the calculated soliton order:

$$o_{\mathrm{sol}}(n_R) = \sqrt{\frac{\gamma A_{\max}^2(n_R)\tau_{\mathrm{FWHM}}^2(n_R)}{|\beta_2| 1.762^2}}.$$

$A_{\max}$ is the peak amplitude, τ_{FWHM} the full width at half maximum of the pulse duration at roundtrip number n_R after dumping. For the fundamental soliton, o_{sol} is equal to 1 and one obtains the area theorem, $A_{\max}\tau_{\mathrm{sech}} = (\beta_2/\gamma)^{1/2}$, using $\tau_{\mathrm{FWHM}}(n_R) = 1.762\ \tau_{\mathrm{sech}}(n_R)$. The black curve represents the peak phase evolution, dotted horizontal and vertical lines indicate a 2π phase step. The deviation from a linear phase is due to the change in pulse energy during one dumping cycle. Immediately after the dumping event with strongly reduced energy the pulse is too short to form a fundamental soliton, thus it sheds away energy into the continuum while broadening. The soliton order reacts with a damped oscillation around the steady state value of 1. The oscillation period asymptotically approaches the phase periodicity known from a fundamental soliton, $n_{\mathrm{phase}} = 2\pi\ \tau^2_{\mathrm{sech}}(n_R) / \beta_2$, as the soliton order gets close to 1. n_{phase} is the number of cavity round-trips during one phase period.

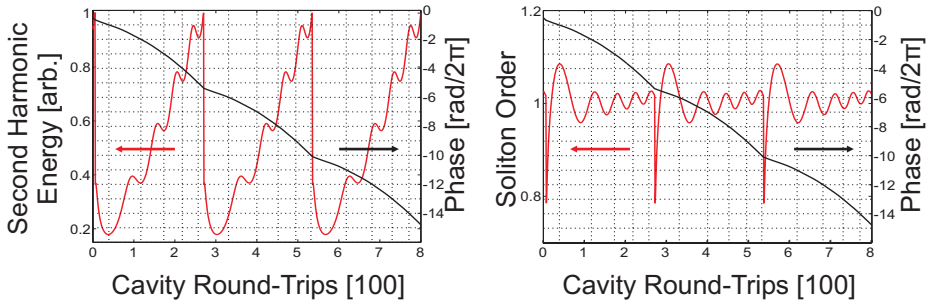

Fig.12. Left: calculated peak power evolution at a dumping rate of 80 kHz in red. Right: calculated transient of the soliton order in red. The pulse peak phase evolution is shown in black in both graphs. The dotted horizontal lines represent 2π-steps on the phase axes. The dotted vertical lines clarify the phase periodicity of the pulse. The distance between two dotted vertical lines indicates the number n_{phase} of cavity round-trips during one phase period. The oscillations in the peak power and in the soliton order asymptotically approach the phase periodicity of the pulse.

#4389 - $15.00 US
Received 17 May 2004; revised 12 July 2004; accepted 13 July 2004

7. Conclusion

In conclusion we have reported on transient effects in a periodically perturbed solitary laser system, namely a Yb:glass femtosecond oscillator with cavity dumping. Measurements on dynamical stability have been conducted and three distinct operational regions, namely a 'relaxed', an 'intermediate', and a 'transient' regime have been identified. In the 'intermediate' regime dynamical instability is present and strong period doubling can be observed; the most stable operation can be obtained either in the 'relaxed' regime with dumping rates of up to 20 kHz, or in the 'transient' regime at frequencies higher than 1 MHz (TR_1 operation). The 'transient' regime has been explored both experimentally and numerically with excellent agreement. The main pulse and spectral shaping mechanisms have been identified as a result of the solitary behavior of the pulse. Two distinct sets of Kelly sidebands have been observed and are due to the main two timescales present in the system: the dumping frequency and the repetition rate of the laser. Based on the better understanding of the physical processes behind, design criteria for improved femtosecond cavity-dumped laser systems can be deduced.

Acknowledgments

The authors thank Jochen Dörring for helpful discussions. Also we thank Max Lederer and Daniel Kopf for the excellent cooperation during development of the laser system. This research was funded by the European union within the contract G1ST-CT-2002-50266.

#4389 - $15.00 US Received 17 May 2004; revised 12 July 2004; accepted 13 July 2004